Published in final edited form as:
Cell Metab. 2012 April 4; 15(4): 480–491. doi:10.1016/j.cmet.2012.03.009.

In vivo identification of bipotential adipocyte progenitors recruited by β3-adrenoceptor activation and high fat feeding

Yun-Hee Lee[1], **Anelia P. Petkova**[1], **Emilio P. Mottillo**[1], and **James G. Granneman**[1,1]

[1]Center for Integrative Metabolic and Endocrine Research, Department of Pathology, Wayne State University School of Medicine, Detroit, MI, 48201

[2]Department of Psychiatry and Behavioral Neuroscience, Wayne State University School of Medicine, Detroit, MI, 48201

Summary

Nutritional and pharmacological stimuli can dramatically alter the cellular phenotypes in white adipose tissue (WAT). Utilizing genetic lineage tracing techniques, we demonstrate that brown adipocytes (BA) that are induced by β3-adrenergic receptor activation in abdominal WAT arise from the proliferation and differentiation of cells expressing platelet-derived growth factor receptor alpha (PDGFRα), CD34 and Sca1 (PDGFRα$^+$ cells). PDGFRα$^+$ cells have a unique morphology in which extended processes contact multiple cells in the tissue microenvironment. Surprisingly, these cells also give rise to white adipocytes (WA) that can comprise up to 25% of total fat cells in abdominal fat pads following 8 weeks of high fat feeding. Isolated PDGFRα$^+$ cells differentiated into both BA and white adipocytes (WA) *in vitro*, and generated WA after transplantation *in vivo*. The identification of PDGFRα$^+$ cells as bipotential adipocyte progenitors will enable further investigation of mechanisms that promote therapeutic cellular remodeling in adult WAT.

Introduction

Adipose tissue is a dynamic organ, whose metabolic phenotype and cellular composition can vary dramatically in response to pharmacological, nutritional, and environmental stimuli (Cinti, 2005). For example, cold exposure or pharmacological activation of β3-adrenergic receptors (ADRB3) induces the appearance of brown adipocytes (BA) in typical white adipose tissue (WAT) depots (Cousin et al., 1992; Young et al., 1984). In addition, high fat feeding expands adipose tissue mass in part by recruiting white adipocytes (WA) from progenitor cells (Gray and Vidal-Puig, 2007; Joe et al., 2009). A substantial body of evidence indicates that adipose tissue dysfunction contributes importantly to the adverse outcomes associated with obesity (Galic et al., 2010), and that recruitment of beneficial cellular phenotypes might offer a means of therapeutic intervention (Sethi and Vidal-Puig, 2007). Thus, an important task to achieving this end is the *in vivo* identification of BA and WA progenitors that are involved in adult WAT cellular plasticity.

Contact: jgranne@med.wayne.edu, phone: 313 577-5629, fax: 313 577-9469.

Most previous approaches to identifying BA and WA progenitors have relied on 'prospective analyses' in which cells are isolated from enzymatically-dissociated tissues by fluorescence-activated cell sorting (FACS), and are demonstrated to have adipogenic potential *in vitro* and *in vivo* following transplantation (Rodeheffer et al., 2008; Schulz et al., 2011; Vegiopoulos et al., 2010). Although these experiments clearly established the existence of cells with adipogenic potential, only *in vivo* lineage tracing can establish which of these populations in fact become BA or WA in response to nutritional and pharmacological stimuli (Kretzschmar and Watt, 2012). In this regard, tracing studies have established that BA in conventional brown adipose depots, such as the interscapular pad, arise from myogenic Myf5+ progenitors, but those induced to appear in WAT do not (Seale et al., 2008). In addition, Tang et al (Tang et al., 2008), traced developmental WA progenitors in typical WAT to cells residing in the vascular mural compartment that express peroxisome profligerator activated receptor gamma (PPARγ) and the pericyte markers platelet-derived growth factor receptor beta (PDGFRβ) and smooth muscle actin (SMA). Perhaps not surprisingly, these cells proliferate and differentiate into WA following treatment of mice with chemical peroxisome proliferator-activated receptor gamma (PPARγ) agonists (Tang et al., 2011) that are used for the treatment of adult-onset diabetes. It is not known whether these cells contribute of brown adipogenesis during adrenergic stimulation or white adipogenesis induced by high fat feeding.

Taking advantage of conditions in which most BA induced by ADRB3 stimulation were derived from proliferating cells, we developed a strategy to identify inducible BA progenitors. Fate tracing of proliferating progenitors tagged with thymidine analogs identified platelet-derived growth factor receptor alpha (PDGFRα) as a likely marker of the BA progenitors. Lineage tracing using constitutive and inducible reporter systems demonstrated that inducible BA (iBA) in WAT were derived from a population of stellate-like cells that express PDGFRα, Sca1 and CD34. Surprisingly, in the absence of ADRB3 stimulation, stellate PDGFRα progenitors differentiated into WA in adult WAT, and this phenomenon was dramatically promoted by high fat feeding. These results define a population of bipotential progenitors that contribute to cellular remodeling in adult WAT.

Results

Recruitment of BA in WAT by ADRB3 stimulation involves depot-specific mechanisms

Previous experiments demonstrated that a significant fraction of BA induced in WAT by ADRB3 stimulation can be derived *de novo* from proliferating progenitors (Granneman et al., 2005). In the present experiments, we investigated the contribution of proliferation to BA induction using a low dose of the ADRB3 agonist CL316,243 (CL) that resulted in greater levels of proliferation without signs of lipolysis-induced inflammation (Granneman et al., 2005; Li et al., 2005; Mottillo et al., 2007). Control and CL-treated mice were coinfused with 5-bromo-2′-deoxyuridine (BrdU) to cumulatively label proliferating cells (Figure 1A and S1A), and the mitotic index and the proportion of BrdU labeling in $UCP1^+$ adipocytes were determined in epididymal (eWAT), inguinal (iWAT) and interscapular (BAT) fat pads.

ADRB3 activation induced expression of UCP1 in iWAT within 3 days of treatment, whereas pronounced expression of UCP1 (i.e., detected by immunoblot) was observed in eWAT only after 7 days. Under control conditions, virtually no $UCP1^+$ cells were detected in WAT, and < 0.4% of nucleated cells incorporated BrdU over 7 days in WAT or BAT (S1B). CL treatment increased the mitotic index of cells in both eWAT and iWAT; however, the mitogenic effect of CL was far greater in eWAT (Figures 1C). The vast majority of $UCP1^+$ cells observed in eWAT were positive for BrdU (82.2 ± 3.6% of total $UCP1^+$ cells, Figures 1D and 1E), indicating most inducible BA (iBA) in eWAT came from newly-born

cells. In contrast, only 5.8 ± 3.0% of $UCP1^+$ cells in iWAT were $BrdU^+$ (Figure 1E). These results indicate that most UCP1+ cells in eWAT are derived from the induction of brown adipogenesis from progenitors, whereas the upregulation of UCP1+ expression in iWAT involves the conversion or 'transdifferentiation' of existing WA into a BA phenotype. Cellular expression levels of UCP1 were similar among UCP+ multilocular cells in interscapular BAT, iWAT and eWAT (Figures 1D, S1C and S1D). CL had no effect on cell proliferation in BAT, further supporting differences in the origin of constitutive and inducible BA. Flash labeling (2 hr) demonstrated that CL treatment produced pronounced proliferation that peaked after 3 days of treatment (Figures 1F and 1G).

Tracking of proliferating cells identifies PDGFRα+ cells as potential iBA progenitors

We next sought to characterize the phenotype of cells that were flash-labeled with EdU after 1, 2, and 3 days of CL treatment (Figure 2A). As detailed below, proliferating cells did not express detectable PDGFRβ, SMA, or CD24, which are found in WA progenitors (Rodeheffer et al., 2008; Tang et al., 2008). The recent report identifying PDGFRα as a marker of ectopic adipocyte progenitors in skeletal muscle (Joe et al., 2010; Uezumi et al., 2010) prompted us to examine PDGFRα expression. $PDGFR\alpha^+$ cells constituted 16.5 ± 0.7% of total cells in control WAT. We found nearly 80% of actively dividing cells expressed PDGFRα after the first day of CL treatment (Figure 2A and 2B). Unexpectedly, a terminal adipocyte differentiation marker, Perilipin1 (PLIN1), was also expressed in numerous EdU flash-labeled (i.e., 2 hr exposure) cells, especially after 3 days of CL treatment. EdU^+ adipocytes were small (< 10 μm) and contained small lipid droplets, indicating that newly-differentiating adipocytes can divide (Pilgrim, 1971). (We have not observed cell division in mature, unilocular adipocytes.) Interestingly, > 90% of EdU^+ cells expressed PDGFRα or PLIN1 (Figure 2B and 2C), but none expressed both markers at the same time (Figure 2A, compare upper and lower panels). Importantly, the frequency of PDGFRα expression in EdU^+ cells declined as PLIN1 expression increased, suggesting that $PDGFR\alpha^+$ progenitors might become $PLIN1^+$ iBA over the course of CL treatment (Figure 2B and 2C). Because the population of $PDGFR\alpha^+$ cells did not change during CL treatment (Figure S2A), it appears that some newly-divided cells replenish the progenitor pool while others down-regulated PDGFRα and differentiated into BA.

To trace the fates of proliferating cells in eWAT, mice were given single injections of EdU on the third day of CL infusion, when proliferation was maximal, and the phenotypic characteristics of EdU-labeled cells were evaluated over time (Figure 2D). Over the 24 h period after flash-labeling, the number of EdU^+ cells expressing PDGFRα progressively decreased as the number of EdU^+ cells expressing PLIN1 increased (Figure 2E-2H), indicating that proliferating cells lose PDGFRα expression as they become fat cells. By 24 h after EdU injection, most proliferating cells were multilocular and expressed PLIN1 (88.1 ± 4.3%) and UCP1 (85.4 ± 3.8%) (Figure 2H).

We performed an additional experiment to trace a relatively pure population of $PDGFR\alpha^+$ cells by labeling cells with EdU on day 1 (Figure S2D). As expected, 88.8±1.8% of EdU^+ cells expressed PDGFRα, and two days later most EdU^+ cells tagged became multilocular brown adipocytes that expressed PPARγ, PLIN1 and UCP1. Interestingly, 16.0 ± 1.6% of EdU^+ cells labeled on day 1 retained PDGFRα expression two days later (Figure S2E and S2G), indicating that $PDGFR\alpha^+$ cells undergo self-renewal as well as adipogenic differentiation. To test whether undifferentiated ($PDGFR\alpha^+$, $PLIN1^-$) and newly-differentiated ($PDGFR\alpha^-$, $PLIN1^+$) cells can undergo multiple divisions, CL-treated mice were injected with EdU on the first day of CL treatment and again with BrdU one day later (Figure S2C). Data from this dual pulse labeling indicated that 48.0 ± 11.3% of EdU^+ $PLIN1^+$ cells (that divided on day 1) were marked by BrdU on day 2 (Figure S2J), demonstrating that a significant number of iBA progenitors divided more than once.

Phenotypic and morphological characteristics of PDGFRα+ progenitors

Confocal imaging of whole mount adipose tissue revealed the unique morphology of PDGFRα$^+$ cells. These cells extended multiple thin cytoplasmic processes (~50μm in length) that were in close proximity to stromal cells, adipocytes and capillaries (Figure 3A, Movie S1). Although sometimes coursing along capillaries, the processes of PDGFRα$^+$ cells extended into the interstitial space (Figure 3A arrows). PDGFRα$^+$ cells were also observed on large diameter blood vessels, however, these cells were not labeled by thymidine analogs, and thus do not contribute directly to brown adipogenesis induced by CL. As mentioned earlier, WA progenitors have been identified as PPARγ$^+$ pericyte-like cells that express SMA and PDGFRβ (Tang et al., 2008). In contrast, adipose tissue PDGFRα$^+$ cells labeled immunochemically or genetically (below) were negative for SMA, PPARγ (Figure 3A). Furthermore, unlike pericytes/adipocyte progenitors, stromal PDGFRα$^+$ cells were larger and did not share a collagen IV basement membrane with endothelial cells as do PDGFRβ$^+$ pericytes (Figure S3). Analysis of eWAT stromal cells by FACS demonstrated that PDGFRα$^+$ cells are a subpopulation of cells expressing the stem cell markers CD34 and Sca1 (Figure 3B), but we did not detect significant coexpression with WA progenitor markers CD24 and PDGFRβ, or the endothelial cell marker isolectin IB4.

Lineage tracing reveals that PDGFRα+ cells become BA during β-adrenergic stimulation

To provide conclusive information on the fate of the PDGFRα expressing progenitors, we performed *in vivo* lineage tracing with two different PDGFRα reporter lines. In one series of experiments, we crossed Cre-responsive (stop codon floxed) reporter mice (Madisen et al., 2010) with mice expressing tamoxifen-inducible CreER^{T2} under the control of PDGFRα promoter (Rivers et al., 2008) (Figure 4A). In this system, treatment of mice with tamoxifen induces expression of tdTomato in PDGFRα$^+$ cells via Cre-mediated recombination. Because the induction is permanent, reporter expression remains in all the cells descending from the originally marked cells.

tdTomato was not observed in the absence of tamoxifen treatment. Tamoxifen induced strong tdTomato fluorescence with high efficiency in adipose tissues (PDGFRα$^+$ tdTomato$^+$/ PDGFRα$^+$ = 57.5 ± 5% in iWAT, 50.4 ± 3% in eWAT). Strong native fluorescence (tdTomato) was uniformly distributed throughout the cells and allowed 3D visualization of their fine structures in whole mount tissues. Consistent with immunostaining analysis, tdTomato-labeled cells were often located in the perivascular region and displayed long thin processes that contacted adjacent adipocytes and vasculature (Figure 4C, Movie S2). Prior to CL treatment, all tdTomato$^+$ cells expressed PDGFRα and CD34 (Figure 4D), but not the developmental WA progenitor markers PPARγ, PDGFRβ, or SMA (Figure 4C).

After 7 days of CL treatment, nearly half of the tdTomato expressing cells had multilocular morphology and expressed BA markers PPARγ, PLIN1, and UCP1 (Figures 4E – 4H). PPARγand PLIN1 are early markers of BA differentiation that were often observed in actively dividing cells. While half of tdTomato$^+$ cells were BrdU$^+$ (Figure 4H), over 90% of tdTomato$^+$ multilocular adipocytes were BrdU$^+$. Conversely, 45 ± 14% of UCP1$^+$ cells in eWAT expressed the tdTomato reporter. Given a reporter recombination efficiency of 50%, we estimate that approximately 90% of iBA in eWAT were derived from proliferating PDFGRα+ cells. As expected from EdU tagging experiments, multilocular tdTomato+ cells lacked expression of PDGFRα (Figure 4E, arrow heads), whereas stellate progenitors remained PDGFRα$^+$ (Figure 4E, arrows). Furthermore, the percentage of tdTomato$^+$ cells that became PLIN1$^+$ adipocytes was 3-fold higher in eWAT compared to iWAT (not shown). Finally, we isolated tdTomato$^+$ cells from control mice and mice treated with CL for 7 days by FACS and examined adipogenic gene expression (Figure 4I). Consistent with immunochemical analyses, CL treatment dramatically upregulated expression of brown

adipocyte markers Ucp1, Elovl3, Dio2 and Cidea. It should be noted that this analysis likely underestimates the effect of CL since floating adipocytes were not recovered.

In a second series of experiments, chromatin-targeted H2BeGFP that was transgenically expressed from the PDGFRα locus (Figure S4A) was used to trace the fate of PDGFRα$^+$ cells in the absence of ongoing PDGFRα expression. Immunohistochemical analysis confirmed that prior to CL treatment, all GFP$^+$ cells expressed PDGFRα and CD34, but not PPARγ, PDGFRβ, or IB4 (Figures S4B and S4C). As expected, nearly 80% of cells induced to divide after 1 day of CL were GFP$^+$, and few of these cells expressed PPARγ (Figures S4E). However, by day 3, 55.3 ± 6.3% of EdU$^+$ cells that divided on day 1 expressed both GFP and PPARγ (Figures S4E and S4F). Multilocular GFP$^+$ cells expressed PLIN1 and UCP1 that were targeted to lipid droplets and mitochondria, respectively (Figures S4F and S4G). It is important to note that these cells were negative for PDGFRα protein and the presence of GFP reflected prior, not current, expression of PDGFRα. Collectively, lineage tracing with two independent genetic marking systems clearly demonstrates that PDGFRα$^+$ cells are BA progenitors within WAT.

Clonal analysis demonstrates that PDGFRα+ cells have BA and WA potential

PDGFRα$^+$ progenitors were isolated by single cell FACS, and individual colonies were expanded and subjected to adipocyte-differentiating conditions (Uezumi et al., 2010) used for establishing adipogenic potential in prospective analyses. Numerous adipocytes were found in more than 70% of clones derived from single cells (Figure 5A). The potential of PDGFRα$^+$ to form colonies and differentiate into adipocytes was similar to that reported for muscle-derived PDGFRα$^+$ cells (Joe et al., 2010; Uezumi et al., 2010). Interestingly, the adipogenic potential of clones derived from eWAT, iWAT and interscapular BAT did not differ significantly (Fisher's exact test, $p > 0.95$). All adipogenic colonies from eWAT contained UCP1+ BA to varying degrees, ranging from 7 to 71% of total adipocytes (n = 29 clones). Figure 5B shows a representative colony stained for lipid and UCP1

We also tested the *in vitro* differentiation potential of PDGFRα$^+$ cells that were isolated from WAT of Pdgfra-H2BeGFP mice by FACS (Figure 5C). Each fraction was expanded under growth conditions, and then exposed to insulin for 7 days to induce adipogenesis. Expanded PDGFRα$^+$ cells retained expression of *Pdgfra*, *Cd34*, *Sca1* (*Ly6a*) and *CD29 (Itgb1)*, but did not express *Pdgfrb* or *Cd24* (Figure 5D). Although both populations formed adipocytes after insulin treatment, the adipogenic potential of PDGFRα$^+$ population was much higher than that of PDGFRα$^-$ population based on the proportion of lipid-laden cells in culture (Figure 5E) and the expression of terminal adipocyte differentiation markers (Figure 5F). This adipogenic induction did not require IBMX and dexamethasone, which are typically used to trigger preadipocyte differentiation. We also evaluated whether differentiated cultures could be induced to express BA markers in response to β-adrenergic stimulation. β-adrenergic stimulation strongly induced expression of peroxisome proliferator-activated receptor γ coactivator 1α (*PGC1α*), *Ucp1* and *Dio2* (Figure 5G), confirming brown adipogenic potential of PDGFRα$^+$ cells *in vitro.*

PDGFRα$^+$ progenitors contribute to adult white adipogenesis during high fat feeding

In vitro analysis indicated that PDGFRα$^+$ cells may become BA or WA, depending on method of induction and level of adrenergic stimulation. To test whether PDGFRα$^+$ cells contribute to white adipogenesis *in vivo*, PDGFRα$^+$ cells were tagged with tdTomato, and mice were maintained on chow or were fed high fat diet (HFD) for 8 weeks. tdTomato-labeled adipocytes were found in isolated small clusters throughout control eWAT pads (Figure 6A). HFD greatly increased the number tdTomato+ adipocytes, which were found in large, extensive clusters throughout eWAT pads (Figure 6A). Immunofluorescence analysis

of paraffin sections confirmed extensive co-expression of PLIN1 in tdTomato+ adipocytes (Figure 6B). Furthermore, all tdTomato+ cells adipocytes of controls and HFD mice were unilocular and none expressed UCP1 (not shown). HFD greatly increased fat tissue mass, and sizing of adipocytes (triglyceride mass/cell) indicated the tissue expansion was mediated largely by adipocyte hypertrophy (Figure 6C). Although there was considerable overlap in adipocyte cellularity between groups (not shown, $p = 0.22$), there was no overlap between chow and HFD mice in the number or density of adipocytes derived from PDGFRα+ cells (Figure 6D, $p < .0002$). Indeed, we estimate that up to 25% of total eWAT adipocytes were derived from PDGFRα$^+$ cells after 8 weeks of HFD versus < 1.8% in controls.

Transplanted FACS-purified PDGFRα$^+$ cells from WAT form WA in vivo

As a final demonstration of the white adipogenic potential of PDGFRα+ progentiors, we transplanted PDGFRα$^+$ and PDGFRα$^-$ cells, purified by FACS from WAT of GFP transgenic mice, into syngenic mice (C57B/6) and determined the efficiency of transplantation 4 weeks later (Figure 7). Matrigel transplants contain a mixture of donor and recipient-derived fat cells (Kawaguchi et al., 1998). The donor contribution, calculated as the fraction of GFP$^+$ adipocytes over total adipocytes in the Matrigel transplant, was 20-fold higher in transplants of PDGFRα$^+$ cells (Figure 7F). Although multilocular adipocytes were detected, none were UCP1$^+$ BA. Moreover, CL treatment 4 weeks after transplantation failed to induce UCP1 expression in transplants (data not shown), implying a crucial role of the endogenous microenvironment in progenitor fate determination. This result further substantiates that PDGFRα$^+$ cells are bipotential progenitors that can give rise to WA or BA.

Discussion

Growing evidence indicates disruption of the interrelated metabolic, endocrine and immune functions of adipose tissue, as occurs during over-nutrition, contributes to risk of diabetes, cardiovascular disease and certain cancers (Khandekar et al., 2011). The fact that the cellular composition and metabolic character of adipose tissue is responsive to nutritional and pharmacologic stimuli (Prins and O'Rahilly, 1997) raises the possibility that adipose tissue plasticity might be targeted for therapeutic benefit (Mottillo and Granneman, 2008; Sun et al., 2011). Nonetheless, the nature of progenitors involved in cellular plasticity of adult WAT *in vivo* is poorly understood.

One potential therapeutic avenue that has been suggested is the expansion of metabolically-desirable BA in typical WAT depots (Tseng et al., 2010; Whittle et al., 2011). We previously reported that at least 20% of multilocular cells in WAT are generated by cell proliferation over 7 days following a standard dose of CL (Granneman et al., 2005). In the present work, we reduced that dose by 75% in order to diminish fatty acid-induced inflammation (Granneman et al., 2005; Mottillo et al., 2007), and found substantially greater proliferation of iBA progenitors in abdominal WAT. Interestingly, nearly all BA in abdominal WAT were derived *de novo*, whereas the vast majority of BA in inguinal fat involved conversion of existing WA to a BA phenotype, as previously proposed (Barbatelli et al., 2010; Cinti, 2009). The immediate progenitors of "convertible" adipocytes in inguinal fat have not been established by tracing techniques, and it is unclear whether these differ from 'inducible' BA in perigonadal fat or whether differences in tissue microenvironment play an important role. Regardless, the rapid proliferation and differentiation of BA progenitors in eWAT provided a strategy to identify and trace their fate *in vivo*.

We established that nearly all proliferating cells marked with EdU after one day of CL treatment expressed PDGFRα, but not previously identified markers of developmental WA progenitors (discussed further below). Three days later, 65% of tagged cells expressed UCP1, strongly indicating that BA are derived from proliferating PDGFRα+ cells. This

conclusion was confirmed using two independent transgenic models that traced the fate of PDGFRα$^+$ proliferating cells. In the first model, tamoxifen-inducible Cre-mediated recombination was used to permanently tag PDGFRα$^+$ cells immediately prior to CL treatment. These experiments provided compelling data demonstrating that ADRB3 stimulation triggers proliferation and differentiation of PDGFRα$^+$ cells into BA. The second model used H2BeGFP expressed from the Pdgfra locus to tag cells with high fidelity and efficiency with a durable marker. Results with this model confirmed that PPARγ$^+$ PLIN1$^+$ multilocular adipocytes are derived from proliferating cells that lose expression of PDGFRα as they differentiate into adipocytes.

PDGFRα$^+$ progenitors represent a subpopulation of stromal cells expressing the common stem cell markers, CD34 and Sca1. ADRB3 stimulation triggered proliferation of PDGFRα$^+$ cells by the first day of CL treatment and generated a transiently amplifying population of progenitors. Although the vast majority of proliferating cells differentiated into BA, a significant fraction of daughter cells retained stem cell characteristics and the progenitor population remained stable over time. Surprisingly, by the third day of CL treatment, the majority of proliferating cells were small, newly-differentiated cells with PLIN1$^+$ lipid droplets. Clearly, growth arrest is not required for differentiation of BA *in vivo* or *in vitro*.

PDGFRα$^+$ progenitors also had WA potential *in vitro*, and contributed to white adipogenesis in adults under control conditions and during high fat feeding. In chow fed mice, tdTomato+ adipocytes were rarely observed as single cells, but rather were nearly always found in clusters, indicating that both WA progenitors likely undergo proliferation prior to differentiation, as do BA progenitors. HFD greatly promoted adipocyte hyperplasia from PDGFRα+ progenitors. By considering steady-state cellularity alone, one might incorrectly conclude that HFD expands fat mass solely by expanding the triglyceride content of existing fat cells. However, inducible tagging, which allows assessment of cellular dynamics, clearly demonstrates significant adipocyte recruitment and possible turnover.

Several groups have isolated distinct cell populations from adipose tissues and muscle that have the potential to form white or brown adipocytes *in vitro* and *in vivo*, following transplantation (Joe et al., 2010; Petrovic et al., 2010; Rodeheffer et al., 2008; Schulz et al., 2011; Uezumi et al., 2010). Although this ‘prospective’ approach clearly identifies cells with adipogenic potential, only lineage tracing can establish which of these potential progenitors, if any, become BA or WA during WAT remodeling *in vivo*. We believe that PDGFRα$^+$ progenitors described here can be distinguished from WA stem cells described by Rodeheffer et al (Rodeheffer et al., 2008) on the basis of tissue abundance and CD24 expression. It seems likely that PDGFRα$^+$ cells were a subpopulation of the Sca1$^+$ cells that were recently shown to be capable of brown adipogenesis (Schulz et al., 2011). However, in contrast to our experiments, cells isolated by these investigators required *ex vivo* treatment with bone morphogen-7 for BA differentiation and these cells were absent in eWAT. Tang, et al. (Tang et al., 2008) utilized lineage tracing techniques to identify direct precursors of WA as cells within the mural compartment that express PPARγ and several pericyte markers. In contrast to those WA progenitors, the PDGFRα$^+$ BA progenitors identified here were negative for PPARγ, SMA, and PDGFRβ, and clearly resided outside of the mural compartment.

PDGFRα$^+$ progenitors are found in numerous tissues where they appear to be involved in cellular repair and restoration (Andrae et al., 2008; Hoch and Soriano, 2003). For example, PDGFRα$^+$ cells may differentiate into fibroblasts or adipocytes in damaged muscle (Joe et al., 2010; Uezumi et al., 2010), depending on the nature of the damage. PDGFRα$^+$ progenitors comprise 5% of cells in brain and contribute to oligodendrocyte formation in adults, and CNS remyelination following injury (Zawadzka et al., 2010). Interestingly, the

three dimensional morphology of brain and adipose PDGFRα$^+$ progenitors is strikingly similar: both extend multiple cellular processes that contact numerous cell types and give the impression of being capable of monitoring the microenvironment (Richardson et al. 2011). In the case of adipose tissue, we suggest that PDGFRα$^+$ cells are adult stem cells that sense metabolic stress or adipogenic signals, and contribute to tissue remodeling and restoration. We anticipate that the *in vivo* identification of PDGFRα$^+$ as bipotential adipocyte progenitors in adult WAT will provide insights into the mechanisms that promote WAT remodeling for therapeutic benefit.

Experimental Procedures

Mice

129S1/SvImJ (129S1; stock no. 002448), C57BL/6J (C57B/6; stock no. 000664), B6.129S4-Pdgfra_tm11(EGFP)Sor/J (Pdgfra-H2BeGFP; stock no. 007669), C57BL/6-Tg(CAG-EGFP)1Osb/J (GFP; stock no. 003292), and B6.Cg-Gt(ROSA)26Sor_tm9(CAG-tdTomato)Hze/J (Madisen et al., 2010) (R26-LSL-tdTomato; stock no. 007909) were purchased from the Jackson Laboratory. Pdgfra-CreER^{T2} mice (Rivers et al., 2008) were obtained from William Richardson (University College London). All animal protocols were approved by the Institutional Animal Care and Use Committee at Wayne State University.

For continuous β-adrenergic stimulation, mice were infused with CL (0.75 nmol/h) by mini-osmotic pumps (ALZET) for up to 7 days. For BrdU cumulative labeling, BrdU (Sigma, 20 μg/h) were infused with CL for 7 days by mini-osmotic pump. For EdU flash-labeling, mice were injected with EdU (Invitrogen, 2 nmol/mouse, I.P.) at indicated time described in the text. For dual pulse labeling, mice were injected first with EdU and then BrdU (2 mg/mouse) with 24 h interval. BrdU was detected by immunostaining, as described below. EdU was detected according to the instructions of the manufacturer (Invitrogen). Intestines from each individual mouse were used as positive controls for EdU or BrdU detection.

Cre recombination in double transgenic mice (Pdgfra-CreERT2/R26-LSL-tdTomato) was induced by administering tamoxifen dissolved in sunflower oil (Sigma, 300 mg/kg, P.O.) on each of 5 consecutive days. CL treatment or HFD were started 1 week after the first dose of tamoxifen. We included no tamoxifen controls to confirm that tdTomato expression is undetectable in the double transgenic mice gavaged with vehicle (oil only). For high fat diet experiment, 60% fat diet (Research Diets D12492) was introduced at 5-6 weeks of age and continued for 8 weeks.

Tissue processing and immunostaining

Tissues were fixed with 10% formalin overnight at 4 °C, embedded in paraffin and cut into 5 μm-thick sections. For whole mounts, fixed tissues were minced into ≤2mm^3 pieces. Immunostaining was performed in either paraffin sections or whole mount tissue. Samples were pre-incubated with permeabilization buffer (0.5% TritonX 100 in PBS) and blocking buffer (5% normal donkey serum in PBS) for 30 min at room temperature, and then incubated sequentially with primary antibody and secondary antibody, all in blocking buffer. For BrdU detection, paraffin sections were incubated in 2 N HCl for 45 min at 37 °C before permeabilization. After washing with TPBS (0.1% Tween 20), samples were counterstained with DAPI. Slides were coverslipped in mounting medium (Dako) and examined by fluorescence microscopy. Species matched IgG were used as nonspecific controls.

Total adipocyte numbers in eWAT of mice from the HFD study were calculated as previously described (Hirsch and Gallian, 1968). Briefly, eWAT adipocyte cell diameters (>300/mouse) were determined from phase-contrast images of fixed whole mounts using IPlab software, and mean triglyceride (TG) mass/adipocyte calculated as = $0.4790/10^6$.

[$3.\sigma^2$. mean diameter + (mean diameter)^3]. Tissue adipocyte cellularity was determined by dividing tissue TG content by mean fat cell TG mass. Total tdTomato+ adipocytes were estimated by extrapolation from the number of cells counted in 10 mg samples.

WAT SVC and adipocyte fractionation

Adipose tissues were washed with PBS, minced and digested with type II collagenase (2 mg/mL) in KRBB containing 10mM HEPES (pH 7.4), and 3% BSA for 1 h at 37 °C. Preparations were passed through a 300 μm mesh, and centrifuged at 500g for 5 minutes. Floating adipocytes were collected by aspiration. Pellets containing the stromal vascular (SV) fraction were incubated in red blood cell lysis buffer for 5 min at room temperature, passed through a 40 μm mesh and then collected by centrifugation at 500 g for 5 min. The resultant cell preparations were subjected to immunostaining or flow cytometry.

Flow cytometry

For FACS analysis, SV fractions from mouse WAT were resuspended in PBS plus 2% FBS, and 0.5mM EDTA. Cells were incubated with anti-PDGFRα (CD140a) -PE, and other cell surface marker antibodies for 30 min on ice (see Supplemental Methods for sources and concentrations). Antibodies used were anti-CD34-FITC, anti-Sca1-FITC, anti-CD24-FITC, and IB4-FITC. For PDGFRβstaining, SV fractions from Pdgfra-H2BeGFP mice were incubated with anti-PDGFRβ (CD140b) -PE. This strategy was adopted because the signals for allophycocyanin-conjugated anti-PDGFRβ antibodies were too low to permit quantification with available anti-PDGFRα antibodies. Species matched IgG were used as nonspecific controls (Figure S3b). For cell sorting, SV cells from GFP mice were labeled with anti-PDGFRα (biotinylated, R&D system) and streptavidin-PE sequentially. SV fractions from Pdgfra-reporter mouse WAT (Pdgfra-H2BeGFP or Pdgfra-CreER^{T2}/R26-tdTomato) were sorted based on native fluorescence (GFP or tdTomato, respectively).

Cell culture of FACS-isolated cells

SVCs of adipose tissue from Pdgfra-H2BeGFP mice were FACS-sorted by GFP fluorescence. Single cells were sorted into individual wells of 96-well plates coated with Martigel. Single colonies were confirmed at < 16 cell stage, and proliferating clones were maintained for 2 weeks in growth medium (DMEM supplemented with 20% FBS and 2.5 ng/ml bFGF). Adipogenic differentiation was induced by incubating cells in DMEM with 20% FBS, 1μg/ml insulin, 0.25μM dexamethasone, and 0.5 mM IBMX. Three days later, clones were place in DMEM with 20% FBS and 1 μg/ml insulin for 4 days. A minimum of 39 colonies derived from the PDGFRα+ single cells from each fat depot was analyzed for the adipogenic differentiation. Colonies were stained for Lipid (LipidTox) to identify adipocytes and UCP1 to identify BA.

In a separate experiment, FACS-purified GFP+ and GFP- cells were collected by centrifugation at 500 g for 5 min, seeded at density of 2.5×10^4/well in 48-well plates, and expanded in growth medium. For adipogenic differentiation, confluent cells were exposed for 7 days to insulin (1 μg/ml) in DMEM supplemented with 10% FBS. For the acute β-adrenergic stimulation, cells were treated with isoproterenol (10 μM) for 4 h.

Transplantation of FACS-isolated cells

FACS-purified PDGFRα$^+$ and PDGFRα$^-$ cells from GFP mice were collected by centrifugation at 500 g for 5 min. For each fraction, 10^5 cells were immediately mixed with Matrigel (150 μl) and injected subcutaneously into the hind limbs of syngenic recipient mice (C57B/6) that were anesthetized with Avertin. Entire transplants were collected after 4 weeks, and stained for PPARγ, PLIN1, or lipid (nile red). Donor cell-derived adipogenesis

in transplants was calculated by the number of GFP^+ adipocytes ($PPAR\gamma^+$ nile red^+) divided by the number of total adipocytes.

Microscopy

Fluorescence and bright-field microscopy was performed using an Olympus IX-81 microscope equipped with a spinning disc confocal unit, and 40× (0.9NA) and 60× (1.2NA) water immersion objectives, using standard excitation and emission filters (Semrock) for visualizing DAPI, FITC (Alexa Fluor 488), Cy3 (Alexa Fluor 555, 594, Nile Red) and Cy5 (Alexa Fluor 647, LipidTox), as described (Granneman et al., 2009). Confocal z-stacks were captured for whole mount tissue by imaging up to 12 optical sections at 0.4-1 μm increments. Raw data of single optical sections (paraffin sections) or confocal z-stacks (whole mount tissues) were processed using IPlabs software (Scanalytics, BD Biosciences) and Adobe Photoshop.

Statistical analysis

Statistical analyses were performed with GraphPad Prism 5. Data are presented as mean ± SEM. Statistical significance between two groups was determined by unpaired t-test or Mann-Whitney test, as appropriate. Comparison among groups was performed using one-way ANOVA or two-way ANOVA, with Bonferroni posttests to determine the relevant p values. Fisher's exact test was used to evaluate differences in cell distributions.

Supplementary Material

Refer to Web version on PubMed Central for supplementary material.

Acknowledgments

We thank Dr. W. Richardson for providing Pdgfra-CreER mice, and Drs. T. Leff, R. MacKenzie and members of CIMER for discussions. This study was supported by NIH grants (RO1DK62292 and RO1DK76629) to JG. The Microscopy, Imaging and Cytometry Resources Core is supported, in part, by NIH Center grant P30CA22453.

References

Andrae J, Gallini R, Betsholtz C. Role of platelet-derived growth factors in physiology and medicine. Genes Dev. 2008; 22:1276–1312. [PubMed: 18483217]

Barbatelli G, Murano I, Madsen L, Hao Q, Jimenez M, Kristiansen K, Giacobino JP, De Matteis R, Cinti S. The emergence of cold-induced brown adipocytes in mouse white fat depots is determined predominantly by white to brown adipocyte transdifferentiation. Am. J. Physiol. Endocrinol. Metab. 2010; 298:E1244–1253. [PubMed: 20354155]

Cinti S. The adipose organ. Prostaglandins, Leukotrienes and Essential Fatty Acids. 2005; 73:9–15.

Cinti S. Transdifferentiation properties of adipocytes in the adipose organ. Am. J. Physiol. Endocrinol. Metab. 2009; 297:E977–E986. [PubMed: 19458063]

Cousin B, Cinti S, Morroni M, Raimbault S, Ricquier D, Penicaud L, Casteilla L. Occurrence of brown adipocytes in rat white adipose tissue: molecular and morphological characterization. J. Cell Sci. 1992; 103:931–942. [PubMed: 1362571]

Galic S, Oakhill JS, Steinberg GR. Adipose tissue as an endocrine organ. Mol. and Cell. Endocrinol. 2010; 316:129–139. [PubMed: 19723556]

Granneman JG, Li P, Zhu Z, Lu Y. Metabolic and cellular plasticity in white adipose tissue I: effects of β3-adrenergic receptor activation. Am. J. Physiol. Endocrinol. Metab. 2005; 289:E608–616. [PubMed: 15941787]

Granneman JG, Moore H-PH, Mottillo EP, Zhu Z. Functional Interactions between Mldp (LSDP5) and Abhd5 in the Control of Intracellular Lipid Accumulation. J. Biol. Chem. 2009; 284:3049–3057. [PubMed: 19064991]

Gray SL, Vidal-Puig AJ. Adipose tissue expandability in the maintenance of metabolic homeostasis. Nutrition reviews. 2007; 65:S7–12. [PubMed: 17605308]

Hirsch J, Gallian E. Methods for the determination of adipose cell size in man and animals. J. Lipid Res. 1968; 9:110–119. [PubMed: 4295346]

Hoch RV, Soriano P. Roles of PDGF in animal development. Development. 2003; 130:4769–4784. [PubMed: 12952899]

Joe AWB, Yi L, Even Y, Vogl AW, Rossi FMV. Depot-Specific Differences in Adipogenic Progenitor Abundance and Proliferative Response to High-Fat Diet. Stem Cells. 2009; 27:2563–2570. [PubMed: 19658193]

Joe AWB, Yi L, Natarajan A, Le Grand F, So L, Wang J, Rudnicki MA, Rossi FMV. Muscle injury activates resident fibro/adipogenic progenitors that facilitate myogenesis. Nat. Cell. Biol. 2010; 12:153–163. [PubMed: 20081841]

Kawaguchi N, Toriyama K, Nicodemou-Lena E, Inou K, Torii S, Kitagawa Y. De novo adipogenesis in mice at the site of injection of basement membrane and basic fibroblast growth factor. Proc. Natl. Acad. Sci. 1998; 95:1062–1066. [PubMed: 9448285]

Khandekar MJ, Cohen P, Spiegelman BM. Molecular mechanisms of cancer development in obesity. Nat. Rev. Cancer. 2011; 11:886–895. [PubMed: 22113164]

Kretzschmar K, Watt Fiona M. Lineage Tracing. Cell. 2012; 148:33–45. [PubMed: 22265400]

Li P, Zhu Z, Lu Y, Granneman JG. Metabolic and cellular plasticity in white adipose tissue II: role of peroxisome proliferator-activated receptor-α. Am. J. Physiol. Endocrinol. Metab. 2005; 289:E617–E626. [PubMed: 15941786]

Madisen L, Zwingman TA, Sunkin SM, Oh SW, Zariwala HA, Gu H, Ng LL, Palmiter RD, Hawrylycz MJ, Jones AR, Lein ES, Zeng H. A robust and high-throughput Cre reporting and characterization system for the whole mouse brain. Nat. Neurosci. 2010; 13:133–140. [PubMed: 20023653]

Mottillo EP, Granneman JG. Therapeutic remodeling of adipose tissue by targeting adipocyte receptors. Cell Science Review. 2008; 5:159–180.

Mottillo EP, Shen XJ, Granneman JG. Role of hormone-sensitive lipase in beta-adrenergic remodeling of white adipose tissue. Am. J. Physiol. Endocrinol. Metab. 2007; 293:E1188–1197. [PubMed: 17711991]

Petrovic N, Walden TB, Shabalina IG, Timmons JA, Cannon B, Nedergaard J. Chronic Peroxisome Proliferator-activated Receptor γ (PPARγ) Activation of Epididymally Derived White Adipocyte Cultures Reveals a Population of Thermogenically Competent, UCP1-containing Adipocytes Molecularly Distinct from Classic Brown Adipocytes. J. Biol. Chem. 2010; 285:7153–7164. [PubMed: 20028987]

Pilgrim C. DNA synthesis and differentiation in developing white adipose tissue. Dev. Biol. 1971; 26:69–76. [PubMed: 5111771]

Prins JB, O'Rahilly S. Regulation of adipose cell number in man. Clin. Sci. (Lond). 1997; 92:3–11.

Rivers LE, Young KM, Rizzi M, Jamen F, Psachoulia K, Wade A, Kessaris N, Richardson WD. PDGFRA/NG2 glia generate myelinating oligodendrocytes and piriform projection neurons in adult mice. Nat. Neurosci. 2008; 11:1392–1401. [PubMed: 18849983]

Rodeheffer MS, Birsoy K, Friedman JM. Identification of White Adipocyte Progenitor Cells In Vivo. Cell. 2008; 135:240–249. [PubMed: 18835024]

Schulz TJ, Huang TL, Tran TT, Zhang H, Townsend KL, Shadrach JL, Cerletti M, McDougall LE, Giorgadze N, Tchkonia T, Schrier D, Falb D, Kirkland JL, Wagers AJ, Tseng Y-H. Identification of inducible brown adipocyte progenitors residing in skeletal muscle and white fat. Proc. Natl. Acad. Sci. 2011; 108:143–148. [PubMed: 21173238]

Seale P, Bjork B, Yang W, Kajimura S, Chin S, Kuang S, Scime A, Devarakonda S, Conroe HM, Erdjument-Bromage H, Tempst P, Rudnicki MA, Beier DR, Spiegelman BM. PRDM16 controls a brown fat/skeletal muscle switch. Nature. 2008; 454:961–967. [PubMed: 18719582]

Sethi JK, Vidal-Puig AJ. Thematic review series: Adipocyte Biology. Adipose tissue function and plasticity orchestrate nutritional adaptation. J. Lipid. Res. 2007; 48:1253–1262. [PubMed: 17374880]

Sun K, Kusminski CM, Scherer PE. Adipose tissue remodeling and obesity. J. Clin. Invest. 2011; 121:2094–2101. [PubMed: 21633177]

Tang W, Zeve D, Seo J, Jo AY, Graff Jonathan M. Thiazolidinediones Regulate Adipose Lineage Dynamics. Cell Metabolism. 2011; 14:116–122. [PubMed: 21723509]

Tang W, Zeve D, Suh JM, Bosnakovski D, Kyba M, Hammer RE, Tallquist MD, Graff JM. White Fat Progenitor Cells Reside in the Adipose Vasculature. Science. 2008; 322:583–586. [PubMed: 18801968]

Tseng Y-H, Cypess AM, Kahn CR. Cellular bioenergetics as a target for obesity therapy. Nat. Rev. Drug. Discov. 2010; 9:465–482. [PubMed: 20514071]

Uezumi A, Fukada S.-i. Yamamoto N, Takeda S.i. Tsuchida K. Mesenchymal progenitors distinct from satellite cells contribute to ectopic fat cell formation in skeletal muscle. Nat. Cell. Biol. 2010; 12:143–152. [PubMed: 20081842]

Vegiopoulos A, Muller-Decker K, Strzoda D, Schmitt I, Chichelnitskiy E, Ostertag A, Diaz MB, Rozman J, Hrabe de Angelis M, Nusing RM, Meyer CW, Wahli W, Klingenspor M, Herzig S. Cyclooxygenase-2 Controls Energy Homeostasis in Mice by de Novo Recruitment of Brown Adipocytes. Science. 2010; 328:1158–1161. [PubMed: 20448152]

Whittle AJ, López M, Vidal-Puig A. Using brown adipose tissue to treat obesity – the central issue. Trends in Mol. Med. 2011; 17:405–411. [PubMed: 21602104]

Young P, Arch JRS, Ashwell M. Brown adipose tissue in the parametrial fat pad of the mouse. FEBS Letters. 1984; 167:10–14. [PubMed: 6698197]

Zawadzka M, Rivers LE, Fancy SPJ, Zhao C, Tripathi R, Jamen F, Young K, Goncharevich A, Pohl H, Rizzi M, Rowitch DH, Kessaris N, Suter U, Richardson WD, Franklin RJM. CNS-Resident Glial Progenitor/Stem Cells Produce Schwann Cells as well as Oligodendrocytes during Repair of CNS Demyelination. Cell Stem Cell. 2010; 6:578–590. [PubMed: 20569695]

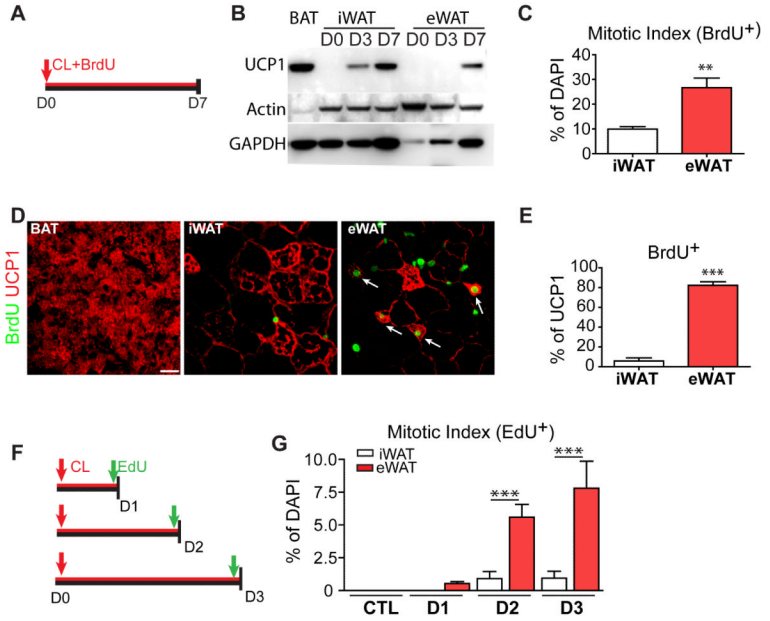

Figure 1. iBA in WAT are derived from proliferating cells during β3- adrenergic stimulation

(A) Cumulative BrdU labeling during continuous CL316,243 (CL) treatment. (B) Immunoblot analysis of WAT from 129S1 mice treated with CL. Equal amounts of proteins were run, and blots sequentially probed for UCP1, and loading controls. (C-E) BrdU incorporation analysis in adipose tissue 7 days after CL treatment. (C) CL induced greater proliferation in eWAT versus iWAT (n = 4 per group, p=0.006). (D) Representative images of BrdU+, UCP1+ cells in tissue paraffin sections with arrows indicating double-positive multilocular adipocytes, (E) Proliferation of iBA in iWAT and eWAT. Values are the percentage of BrdU+,UCP1+ to total UCP1+ cells. (mean ± SEM, n = 4 per group, p<0.0001). (F) EdU flash-labeling. 129S1 mice were infused with CL up to 3 days and injected with EdU 2 h before analysis. (G) CL significantly increased mitotic indices of both eWAT and iWAT (p<0.0001), and the effect was significantly greater in eWAT versus iWAT (ANOVA interaction p=0.0033, post-test ***p<0.001) (mean ± SEM, n = 3-4 per group). See also Figure S1.

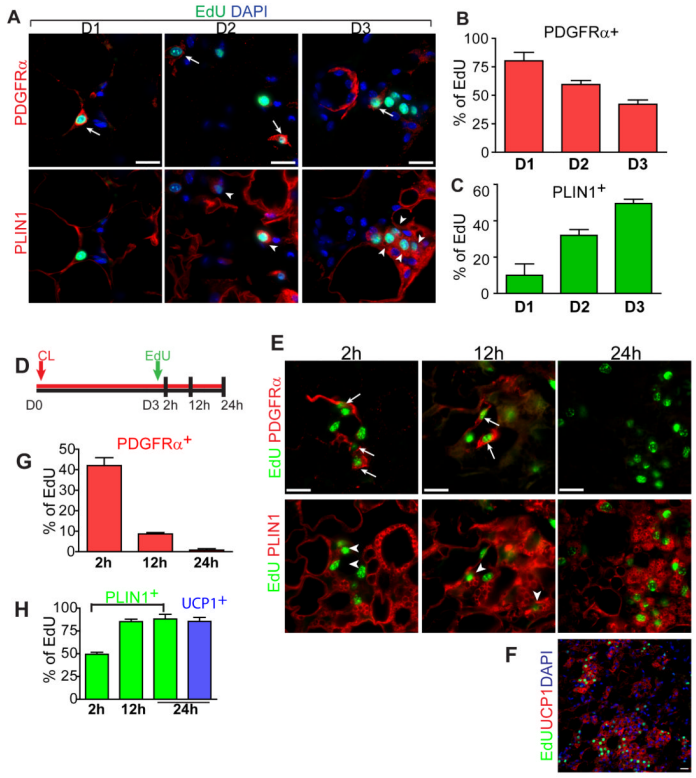

Figure 2. Fate tracing of proliferating cells identifies PDGFRα+ cells as potential iBA progenitors

(A) Representative images of eWAT paraffin sections triple-stained for PDGFRα, PLIN1 and EdU on D1, D2, or D3 of CL treatment. Note that images of a given day are the same microscopic field. Top row shows merge of PDGFRα (red) and EdU (green), while bottom row is merge of PLIN1 (red) and EdU (green). Arrows mark PDGFRα+ EdU+ cells. Arrow heads mark PLIN1+ EdU+ cells. Nuclei were counterstained with DAPI (Blue). Triply stained images demonstrate that PLIN1 and PDGFRα expression are mutually exclusive. (B, C) Quantification of PDGFRα+ EdU+ cells, or PLIN1+ EdU+ cells in eWAT paraffin sections (mean ± SEM, n = 3-4 per group). Nearly all proliferating cells in eWAT express either PDGFRα or PLIN1. The percentage of PLIN1+, EdU+ cells increased over time (B, p=0.0004) as the percentage of PDGFRα+, Edu+ cells declined (C, p=0.002). (D) Fate tracing of cells labeled with EdU on the third day of CL treatment. 129S1 mice were infused with CL, injected with EdU on D3, and analyzed at indicated time points. (E) Representative images of eWAT paraffin sections triple-stained for PDGFRα, PLIN1 and EdU at 2 h, 12 h, and 24 h after EdU injection. Top row shows merge of PDGFRα (red) and EdU (green), while bottom row is merge of PLIN1 (red) and EdU (green) of the same field. Arrows mark PDGFRα+ EdU+ cells. Arrow heads mark PLIN1+ EdU+ cells. (F) Low magnification fields of eWAT paraffin sections double-stained for EdU (green) and UCP1 (red) at 24h after EdU injection. (G, H) Proportion of each cell type is expressed as percentage of the total EdU+ cells (mean ± SEM, n = 3-4 per group). PDGFRα expression declined (p=0.0002) as PLIN1 expression appeared (p=0.0001) in EdU-labeled cells. By 24 h, 85% of EdU+ cells expressed UCP1. Bars = 20 μm. See also Figure S2.

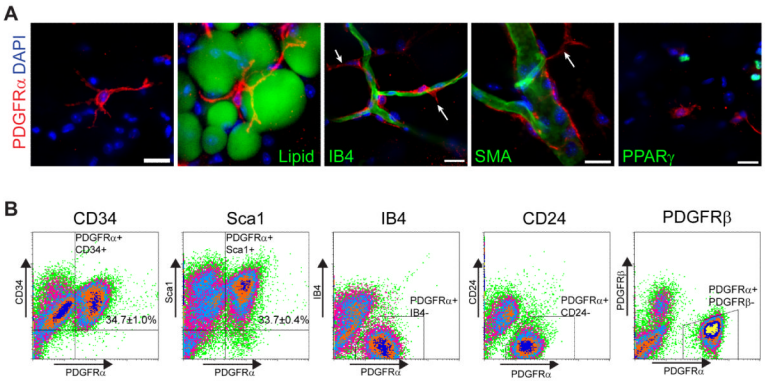

Figure 3. Phenotypic and morphological characteristics of PDGFRα$^+$ cells

(A) Immunostaining of PDGFRα+ cells in eWAT whole mount from control 129S1 mice. (A) Stellate morphology of PDGFRα+ cells (red). Each cell had multiple processes, some up to 50 μm long, and contacted multiple cells, including adipocytes (Lipid+). PDGFRα+ cells were often in close apposition to IB4+ vasculature (green), but did not constitute the mural compartment, indicated by extended processes (arrows). PDGFRα+ cells were negative for SMA and PPARγ. Nuclei were counterstained with DAPI. Bars = 20 μm. (B) FACS analysis on cell surface marker expression of PDGFRα+ cells. PDGFRα+ cells were uniformly positive for CD34 and Sca1, but negative for IB4, CD24, and PDGFRβ. The percentage of double positive cells are indicated on the flow profile (mean ± SEM, n = 3 independent analyses). See also Figure S3 and Movie S1.

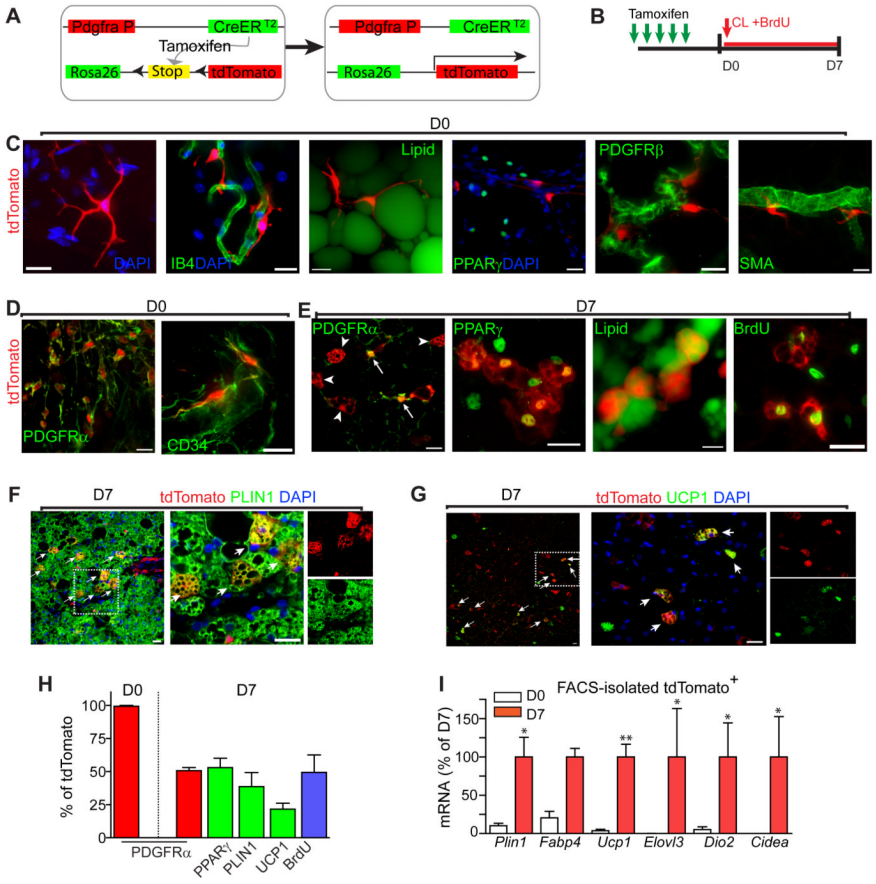

Figure 4. PDGFRα expressing progenitors become BA during β3-adrenergic stimulation

(A) Schematic diagram of the inducible Pdgfra-CreERT2/R26-LSL-tdTomato reporter system. (B) Procedure of reporter induction and lineage tracing of tdTomato-labeled cells. Efficiency and specificity of reporter induction were analyzed 7 days after the first tamoxifen dose. Adipose tissue was analyzed before (D0) or 7 days (D7) after CL and BrdU infusion. (C,D) Characterization of reporter+ cells prior to CL treatment. Labeled cells were often found near blood vessels (IB4+) and had long processes that appeared to contact stromal cells and adipocytes (LipidTox+). tdTomato+ cells were negative for PPARγ, PDGFRβ, and SMA, but uniformly positive for PDGFRα and CD34. (E-G) Characterization of reporter+ cells following 7 days of CL treatment. tdTomato+ multilocular adipocytes (arrow heads) lacked expression of PDGFRα, whereas stellate-like progenitors (arrows) remained PDGFRα^{+}. tdTomato+ multilocular cells coexpressed PPARγ, UCP1, and contained PLIN1^{+} lipid droplets. Incorporation of BrdU of tdTomato+ multilocular adipocytes indicates that iBA came from proliferating cells. (F, G) Low magnification images of eWAT paraffin sections double stained for tdTomato and PLIIN1 (F), or UCP1 (G). Arrows mark double positive cells. Right is a magnified view of the boxed region from left. Bars = 20 μm. (H) Distribution of markers in tdTomato+ cells (mean ± SEM, n = 3 per group). All tdTomato+ cells expressed PDGFRα and none expressed PPARγ on day 0. By day 7, 47.3 ± 1.5% of tdTomato+ cells retained expression of PDGFRα while 44.3 ± 14.6 % of tdTomato+ cells expressed PPARγ (Fisher's exact test, $p<0.0001$). In addition, PLIN1 (38.7 ± 10.6%) and UCP1 (21.5 ± 4.4%) expression and BrdU incorporation (49.3 ± 13.2) were detected in tdTomato+ cells. (I) qPCR analysis of BA marker expression in Pdgfra-tdTomato tagged cells isolated by FACS, expressed relative mRNA levels of D7. BA markers were significantly upregulated in tdTomato+ cells after 7 days of CL treatment.

(mean ± SEM, n = 4-5, *Plin1*: p=0.016, fatty acid bind protein 4 *(Fabp4)*: p=0.057, *UCP1*: p=0.008, and *Elovl3*: p=0.029, *Dio2*: p=0.033, *Cidea*: p=0.011). See also Figure S4 and Movie S2.

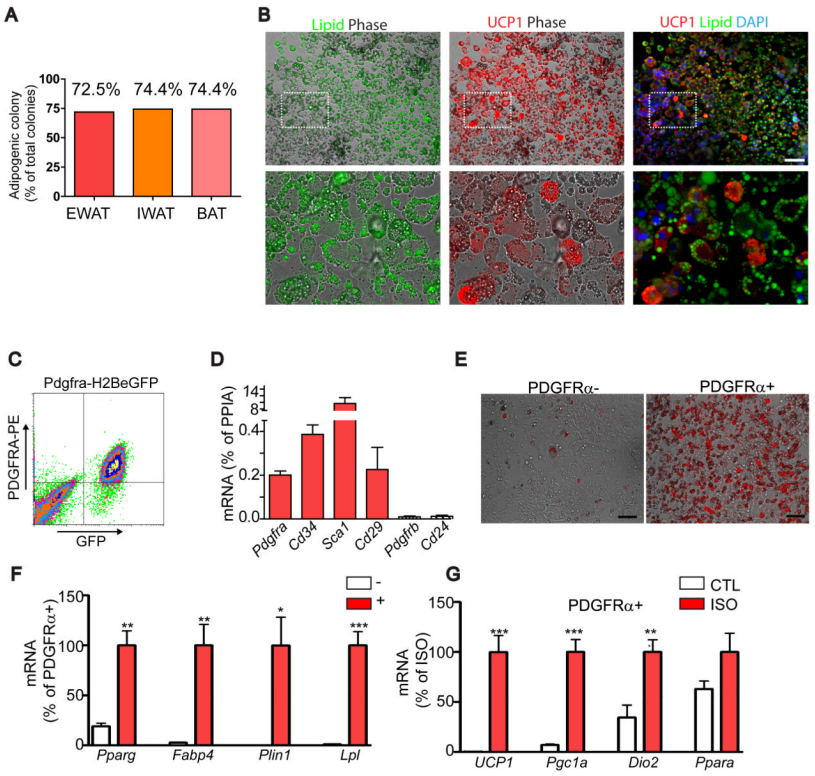

Figure 5. PDGFRα-expressing progenitors are white and brown adipogenic *in vitro*

(A-B) Adipogenic potential of clones (n > 39) derived from FACS-isolated PDGFRα+ single cells. (B) Representative images of adipogenic clones double-stained for UCP1 and Lipid (LipidTox). Lipid (left) and UCP1 (middle) fluorescent images were merged with phase contrast, and Lipid and UCP1 images were merged wth DAPI-counterstained images. Bottom row is a magnified view of the boxed regions from top row. All adipogenic clones contained UCP1+ and UCP1- adipocytes, demonstrating WA and BA bipotentiality of PDGFRα+ progenitors. Bar = 100 μm. (C) FACS analysis of H2BeGFP+ (PDGFRα+) cells from WAT. (D) qRT-PCR analysis of surface marker expression after 5-7 days of culture in growth medium (means ± SEM, n=4). (E) Representative images of PDGFRα+ or PDGFRα- cells cultured in the presence of insulin (1μg/mL) for 7 days. Boron-dipyrromethene (BODIPY, red) staining indicates higher insulin-stimulated adipogenesis in PDGFRα^{+} fractions. (H, I) qRT-PCR analysis on adipocyte gene expression. (F) Expression of adipocyte-specific markers, normalized to that of PDGFRa+ cells. PDGFRα+ cells were significantly more responsive to insulin-induced adipogenesis, compared to PDGFRα- cells (means ± SEM, n=4, *Pparg*: p=0.002, *Fabp4*: p=0.004, *Plin1*: p=0.012, and *lipoprotein lipase (Lpl)*: p=0.0003). (G) Expression of brown adipocyte-specific markers, normalized to levels induced by ISO. Differentiated PDGFRα+ populations (cultured in the presence of Insulin for 7 days) were treated with vehicle (CTL) or isoproterenol (ISO, 10 μM) for 4 h before analysis. (means ± SEM, n=4, *Ucp1*: p=0.0009, *Pgc1*: p=0.0003, *Dio2:* p=0.0095, *Ppara*: p=0.120). Experiments were repeated 4 times.

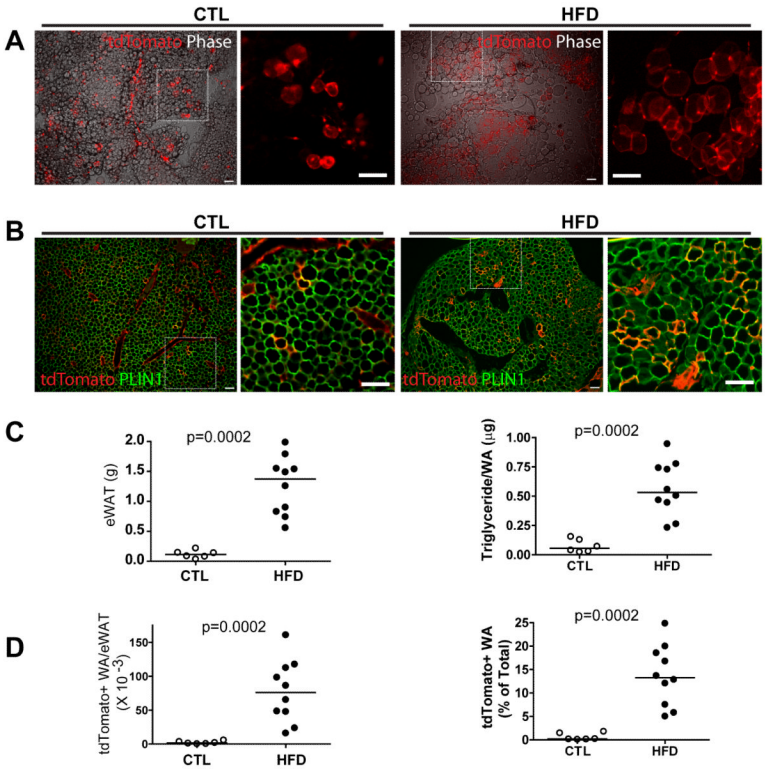

Figure 6. PDGFRα^{+} progenitors contribute to adult white adipogenesis under control conditions and during adipose tissue expansion induced by high fat feeding

(A) Representative images of tdTomato+ cells in eWAT whole mount from control and HFD mice. tdTomato fluorescent images are merged with phase contrast (left) along with a magnified region illustrating tdTomato+ adipocyte clusters (right). (B) Representative images of eWAT paraffin sections double-stained for tdTomato and PLIN1. Images demonstrate abundance of tdTomato+ adipocytes in eWAT from HFD mice. (C) Effect of HFD on the weight of eWAT pads (left) and adipocyte triglyceride content (right). (d) The density of tdTomato+ adipocytes in these pads of mice on chow and HFD. The number of tdTomato+ cells was estimated in eWAT pads and proportion of tdTomato+ adipocytes is expressed as percentage of the total adipocytes. Bar = 100 μm.

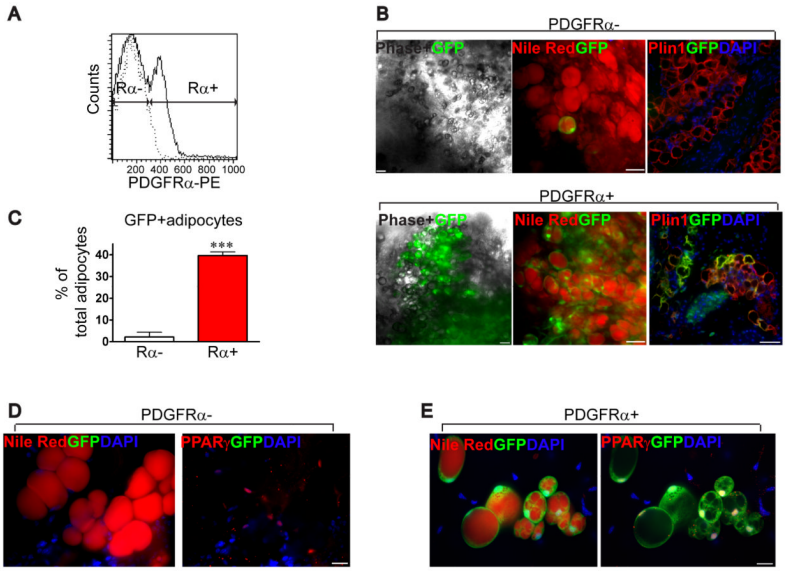

Figure 7. *In vivo* adipogenic potential of FACS-purified PDGFRα expressing progenitors

(A) FACS analysis of PDGFRα+ cells from WAT of GFP transgenic mice. The X-axis indicates PE intensity (PDGFRα expression). Histogram with dashed line represents the negative control for PDGFRα staining. (B) Representative low magnification images of engrafted PDGFRα+ or PDGFRα- cells in Matrigel 4 weeks after transplantation. Bars = 50 μm. GFP (green) fluorescent images were merged with phase contrast (left), nile red fluorescence (middle, red) or Plin1 immunofluorescence (right, red). Images demonstrate abundance of GFP+ adipocytes in PDGFRα+ transplants by native fluorescence in whole mount tissue (left and middle) and by immunostaining on paraffin sections (right). Nuclei were counterstained with DAPI. (C) Quantitative analysis of GFP+ adipocytes. Donor contribution is the percentage of total adipocytes (nile red+, PPARγ+) from the transplant that were donor-derived (GFP+). Values are means ± range for 2 independent experiments ($p<0.0001$, Fisher's exact test). (D-E) High magnification images of nile red (left, red) and PPARγ (right, red) in whole mount tissues. Bars = 20 μm.